

Westinghouse Non-Proprietary Class 3

WCAP- 16311-NP
Revision 0

August 2004

Technical Justification for Eliminating Pressurizer Surge Line Rupture as the Structural Design Basis for the R. E. Ginna Nuclear Power Plant

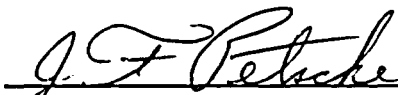


WCAP-16311-NP Revision 0

Technical Justification for Eliminating Pressurizer Surge Line Rupture as the Structural Design Basis for the R. E. Ginna Nuclear Power Plant

D. C. Bhowmick

August 2004

Verified: 
J. F. Petsche
Piping Analysis and Fracture Mechanics

Approved: 
S. A. Swamy, Manager
Piping Analysis and Fracture Mechanics

Westinghouse Electric Company LLC
P.O. Box 355
Pittsburgh, PA 15230-0355

© 2004 Westinghouse Electric Company LLC
All Rights Reserved

TABLE OF CONTENTS

LIST OF TABLES	v
LIST OF FIGURES	vi
1 INTRODUCTION.....	1-1
1.1 Background.....	1-1
1.2 Scope and Objective	1-1
1.3 References.....	1-2
2 OPERATION AND STABILITY OF THE PRESSURIZER SURGE LINE AND THE REACTOR COOLANT SYSTEM.....	2-1
2.1 Stress Corrosion Cracking.....	2-1
2.2 Water Hammer.....	2-2
2.3 Low Cycle and High Cycle Fatigue.....	2-2
2.4 Summary Evaluation of Surge Line for Potential Degradation During Service.....	2-3
2.5 Reference	2-3
3 MATERIAL CHARACTERIZATION.....	3-1
3.1 Pipe Material And Welding Process.....	3-1
3.2 Material Properties	3-1
3.3 Reference	3-1
4 LOADS FOR FRACTURE MECHANICS ANALYSIS	4-1
4.1 Nature of The Loads.....	4-1
4.2 Loads For Crack Stability Analysis.....	4-2
4.3 Loads For Leak Rate Evaluation	4-2
4.4 Loading Conditions.....	4-2
4.5 Summary of Loads	4-3

4.6	Governing Locations	4-4
5	FRACTURE MECHANICS EVALUATION.....	5-1
5.1	Global Failure Mechanism.....	5-1
5.2	Leak Rate Predictions	5-2
5.2.1	General Considerations.....	5-2
5.2.2	Calculation Method.....	5-2
5.2.3	Leak Rate Calculations.....	5-3
5.3	Stability Evaluation	5-3
5.4	References.....	5-4
6	ASSESSMENT OF FATIGUE CRACK GROWTH	6-1
6.1	Methodology.....	6-1
6.2	Results	6-2
6.3	References	6-2
7	ASSESSMENT OF MARGINS.....	7-1
8	CONCLUSIONS	8-1
	APPENDIX A - LIMIT MOMENT	A-1

LIST OF TABLES

Table 3-1	Room Temperature Mechanical Properties of the Pressurizer Surge Line Materials.....	3-2
Table 3-2	Representative Tensile Properties of the Pressurizer Surge Line Material.....	3-3
Table 3-3	Modulus of Elasticity (E) of the Pressurizer Surge Line Material.....	3-3
Table 4-1	Types of Loadings	4-4
Table 4-2	Normal and Faulted Loading Cases for Leak-Before-Break Evaluations	4-5
Table 4-3	Associated Load Cases for LBB Analyses.....	4-6
Table 4-4	Summary of Leak-Before-Break Loads And Stresses at the Three Highest Stressed Weld Locations	4-7
Table 5-1	Summary of Leakage Flaw Sizes	5-5
Table 5-2	Summary of Critical Flaw Sizes.....	5-5
Table 6-1	Fatigue Crack Growth Results for Initial flaw Size of 10% of the Wall Thickness	6-3
Table 7-1	Leakage Flaw Sizes, Critical Flaw Sizes and Margins	7-2
Table 7-2	Leak-Before-Break Conservatisms.....	7-2

LIST OF FIGURES

Figure 3-1	R. E. Ginna Nuclear Power Plant Surge Line Layout.....	3-4
Figure 4-1	R. E. Ginna Nuclear Power Plant Surge Lines Showing Analyzed Weld Locations by Node Point.....	4-8
Figure 5-1	Fully Plastic Stress Distribution	5-6
Figure 5-2	Analytical Predications of Critical Flow Rates of Steam-Water Mixtures	5-7
Figure 5-3	[ρ_a, ρ_c, ρ_e Pressure Ratio as a Function of L/D.....	5-8
Figure 5-4	Idealized Pressure Drop Profile through a Postulated Crack.....	5-9
Figure 5-5	Loads acting on the Model at the Governing Locations	5-10
Figure 5-6	Critical Flaw Size Prediction for Node 1020 Case D.....	5-11
Figure 5-7	Critical Flaw Size Prediction for Node 1020 Case E	5-12
Figure 5-8	Critical Flaw Size Prediction for Node 1020 Case F	5-13
Figure 5-9	Critical Flaw Size Prediction for Node 1120 Case D	5-14
Figure 5-10	Critical Flaw Size Prediction for Node 1120 Case E	5-15
Figure 5-11	Critical Flaw Size Prediction for Node 1120 Case F	5-16
Figure 5-12	Critical Flaw Size Prediction for Node 1280 Case D.....	5-17
Figure 5-13	Critical Flaw Size Prediction for Node 1280 Case E	5-18
Figure 5-14	Critical Flaw Size Prediction for Node 1280 Case F	5-19
Figure 6-1	Orientation of Angular Locations for the Fatigue Crack Growth Analysis.....	6-4
Figure 6-2	Reference Fatigue Crack Growth Curves for Austenitic Stainless Steel in Air Environments	6-5
Figure A-1	Pipe with a Through-wall Crack In Bending.....	A-2

1 INTRODUCTION

1.1 BACKGROUND

The current pressurizer surge line Leak-Before-Break analysis is documented in RGE-02-004 Revision 0 (Reference 1-1) and approved by the NRC (Reference 1-2). Reference 1-1 analysis did not consider the effects of thermal stratification since the thermal stratification phenomenon in the surge line was not a concern at that time. The pressurizer surge line is known to be subjected to thermal stratification and the effects of thermal stratification for the R. E. Ginna Nuclear Power Plant surge line have been evaluated and documented in WCAP-12928 (Reference 1-3). The purpose of this report is to document the Leak-Before-Break analysis for the Ginna pressurizer surge considering the effects of the thermal stratification.

The results of the stratification evaluation as described in WCAP-12928 have been used in the Leak-Before-Break analysis presented in this report. Presented in this report are the descriptions of a mechanistic pipe break evaluation method and the analytical results that can be used for establishing that a circumferential type break will not occur within the pressurizer surge line. The evaluations consider that circumferentially oriented flaws cover longitudinal cases.

1.2 SCOPE AND OBJECTIVE

The purpose of this investigation is to demonstrate Leak-Before-Break (LBB) for the R. E. Ginna Nuclear Power Plant pressurizer surge line. The scope of this work covers the entire pressurizer surge line from the primary loop nozzle junction to the pressurizer nozzle junction. A schematic drawing of the surge line piping system is shown in Section 3.0. The recommendations and criteria proposed in SRP 3.6.3 (Reference 1-4) are used in this evaluation. The criteria and the resulting steps of the evaluation procedure can be briefly summarized as follows:

1. Calculate the applied loads. Identify the location at which the highest faulted stress occurs.
2. Identify the materials and the material properties.
3. Postulate a through-wall flaw at the governing location(s). The size of the flaw should be large enough so that the leakage is assured of detection with margin using the installed leak detection equipment, when the pipe is subjected to normal operating loads. Demonstrate that there is a margin of 10 between the calculated leak rate and the leak detection capability.
4. Using maximum faulted loads in the stability analysis, demonstrate that there is a margin of 2 between the leakage size flaw and the critical size flaw.

5. Review the operating history to ascertain that operating experience has indicated no particular susceptibility to failure from the effects of corrosion, water hammer or low and high cycle fatigue.
6. For the materials types used in the plant, provide representative material properties.
7. Demonstrate margin on applied load.
8. Perform an assessment of fatigue crack growth. Show that a through-wall crack will not result.

The leak rate is calculated for the normal operating condition. The leak rate prediction model used in this evaluation is an [

ja,c,e. The crack opening area required for calculating the leak rates is obtained by (Reference 1-5) subjecting the postulated through-wall flaw to normal operating loads. Surface roughness is accounted for in determining the leak rate through the postulated flaw.

It should be noted that the terms "flaw" and "crack" have the same meaning and are used interchangeably. "Governing location" and "critical location" are also used interchangeably throughout the report.

1.3 REFERENCES

- 1-1 RGE-02-004 Revision 0," Fracture Mechanics Evaluation of High Energy Piping Lines at the R. E. Ginna Nuclear Power Plant, April 8 1983. (Prepared by Nutech Engineers, San Jose, California).
- 1-2 NRC Docket No. 50-244, LS05-83-06-062, "IPSAR Section 4.13, Effects of Pipe Break on Structures, Systems and Components Inside Containment for the R. E. Ginna Nuclear Power Plant, " June 28, 1983.
- 1-3 WCAP-12928, "Structural Evaluation of the Robert E. Ginna Pressurizer Surge line, Considering the Effects of Thermal Stratification," May 1991. (Westinghouse Proprietary).
- 1-4 Standard Review Plan; public comments solicited; 3.6.3 Leak-Before-Break Evaluation Procedures; Federal Register/Vol. 52, No. 167/Friday, August 28, 1987/Notices, pp. 32626-32633.
- 1-5 Tada, H., "The Effects of Shell Corrections on Stress Intensity Factors and the Crack Opening Area of Circumferential and a Longitudinal Through-Crack in a Pipe," Section II-1, NUREG/CR-3464, September 1983.

2 OPERATION AND STABILITY OF THE PRESSURIZER SURGE LINE AND THE REACTOR COOLANT SYSTEM

2.1 STRESS CORROSION CRACKING

The Westinghouse reactor coolant system primary loop and connecting Class 1 lines have an operating history that demonstrates the inherent operating stability characteristics of the design. This includes a low susceptibility to cracking failure from the effects of corrosion (e.g., intergranular stress corrosion cracking, IGSCC). This operating history totals over 1100 reactor-years, including 5 plants each having over 30 years of operation, 4 plants each with over 25 years of operation, 12 plants each with over 20 years of operation and 8 plants each with over 15 years of operation.

For stress corrosion cracking (SCC) to occur in piping, the following three conditions must exist simultaneously: high tensile stresses, susceptible material, and a corrosive environment. Since some residual stresses and some degree of material susceptibility exist in any stainless steel piping, the potential for stress corrosion is minimized by properly selecting a material immune to SCC as well as preventing the occurrence of a corrosive environment. The material specifications consider compatibility with the system's operating environment (both internal and external) as well as other material in the system, applicable ASME Code rules, fracture toughness, welding, fabrication, and processing.

The elements of a water environment known to increase the susceptibility of austenitic stainless steel to stress corrosion are: oxygen, fluorides, chlorides, hydroxides, hydrogen peroxide, and reduced forms of sulfur (e.g., sulfides, sulfates, and thionates). Strict pipe cleaning standards prior to operation and careful control of water chemistry during plant operation are used to prevent the occurrence of a corrosive environment. Prior to being put into service, the piping is cleaned internally and externally. During flushes and preoperational testing, water chemistry is controlled in accordance with written specifications. Requirements on chlorides, fluorides, conductivity, and pH are included in the acceptance criteria for the piping.

During plant operation, the reactor coolant water chemistry is monitored and maintained within very specific limits. Contaminant concentrations are kept below the thresholds known to be conducive to stress corrosion cracking with the major water chemistry control standards being included in the plant operating procedures as a condition for plant operation. For example, during normal power operation, oxygen concentration in the RCS and connecting Class 1 line is expected to be in the ppb (parts per billion) range by controlling charging flow chemistry and maintaining hydrogen in the reactor coolant at specified concentrations. Halogen concentrations are also stringently controlled by maintaining concentrations of chlorides and fluorides within the specified limits. This is assured by controlling charging flow chemistry. Thus during plant operation, the likelihood of stress corrosion cracking is minimized.

Wall thinning by erosion and erosion-corrosion effects will not occur in the surge line due to the low velocity and the material, austenitic stainless steel, is highly resistant to these degradation mechanisms. Therefore, wall thinning is not a significant concern in the portion of the system being addressed in this evaluation.

As a result of the recent issue of Primary Water Stress Corrosion Cracking (PWSCC) occurring in V. C. Summer reactor vessel hot leg nozzle, Alloy 82/182 weld is being currently investigated under the EPRI Materials Reliability Project (MRP) Program. It should be noted that the susceptible material under investigation is not found in the pressurizer surge line piping at the R. E. Ginna Nuclear Power Plant.

2.2 WATER HAMMER

Overall, there is a low potential for water hammer in the RCS and the connecting surge line since they are designed and operated to preclude the voiding condition in the normally filled surge line. The RCS and connecting surge line including piping and components, are designed for normal, upset, emergency, and faulted condition transients. The design requirements are conservative relative to both the number of transients and their severity. Pressurizer safety and relief valve actuation and the associated hydraulic transients following valve opening are considered in the system design. Only relatively slow transients are applicable to the surge line and there is no significant effect on the system dynamic loads. To ensure dynamic system stability, reactor coolant parameters are stringently controlled. Temperature during normal operation is maintained within a narrow range by the control rod positions. Pressure is also controlled within a narrow range for steady-state conditions by the pressurizer heaters and the pressurizer spray. The flow characteristics of the system remain constant during a fuel cycle because the only governing parameters, namely system resistance and the reactor coolant pump characteristics, are controlled in the design process. Additionally, Westinghouse has instrumented typical reactor coolant systems to verify the flow and vibration characteristics of the system and the connecting auxiliary lines. Preoperational testing and operating experience have verified the Westinghouse approach. The operating transients of the RCS primary piping and the connected surge line are such that no significant water hammer can occur.

2.3 LOW CYCLE AND HIGH CYCLE FATIGUE

Fatigue considerations are accounted for in the surge line piping through the fatigue usage factor evaluation for the stratification analyses (Reference 1-3) to show compliance with the rules of Section III of the ASME Code. A further assessment of the low cycle fatigue loading is discussed in Section 6.0 as part of this study in the form of a fatigue crack growth evaluation.

Pump vibrations during operation would result in high cycle fatigue loads in the piping system. During operation, an alarm signals the exceeding of the RC pump vibration limits. Field measurements have been made on the reactor coolant loop piping in a number of Plants during hot functional testing. Stresses in the elbow below the RC pump have been found to be very small, between 2 and 3 ksi at the highest. Field measurements on a typical PWR plant indicate vibration amplitudes less than 1 ksi. When translated to the connecting surge line, these stresses would be even lower, well below the fatigue endurance limit for the surge line material and would result in an applied stress intensity factor below the threshold for fatigue crack growth. R. E. Ginna configurations are similar and the results are expected to be the similar.

2.4 SUMMARY EVALUATION OF SURGE LINE FOR POTENTIAL DEGRADATION DURING SERVICE

There has never been any service cracking or wall thinning identified in the pressurizer surge line of Westinghouse PWR design. The design, construction, inspection, and operation of the pressurizer surge line piping mitigate sources of such degradation.

There is no known mechanism for water hammer in the pressurizer/surge system. The pressurizer safety and relief piping system that is connected to the top of the pressurizer could have loading from water hammer events. However, these loads are effectively mitigated by the pressurizer and have a negligible effect on the surge line.

Wall thinning by erosion and erosion-corrosion effects should not occur in the surge line due to the low velocity, typically less than 1.0 ft/sec and the material, austenitic stainless steel, which is highly resistant to these degradation mechanisms. Per NUREG-0691 (Reference 2-1), a study on pipe cracking in PWR piping reported only two incidents of wall thinning in stainless steel pipe and these were not in the surge line. The cause of wall thinning is related to the high water velocity and is therefore clearly not a mechanism that would affect the surge line.

It is well known that the pressurizer surge line is subjected to thermal stratification and the effects of stratification are particularly significant during certain modes of heatup and cooldown operation. The effects of stratification have been evaluated for the R. E. Ginna Nuclear Power Plant surge line and the loads, accounting for the stratification effects, have been derived in WCAP-12928 (Reference 1-3). These loads are used in the Leak-Before-Break evaluation described in this report.

The R. E. Ginna Nuclear Power Plant surge line piping system is fabricated from forged products (see Section 3) which are not susceptible to toughness degradation due to thermal aging.

Finally, the maximum operating temperature of the pressurizer surge line piping, which is about 650°F, is well below the temperature that would cause any creep damage in stainless steel piping. Cleavage type failures are not a concern for the operating temperatures and the material used in the stainless steel piping of the pressurizer surge line.

2.5 REFERENCE

- 2-1 Investigation and Evaluation of Cracking Incidents in Piping in Pressurized Water Reactors, NUREG-0691, U.S. Nuclear Regulatory Commission, September 1980.

3 MATERIAL CHARACTERIZATION

3.1 PIPE MATERIAL AND WELDING PROCESS

The pipe material of the pressurizer surge line for the R. E. Ginna Nuclear Power Plant is SA376 TP316. This is a wrought product of the type used for the piping of several PWR Plants. The surge line is connected to the primary loop at one end and at the other end to the pressurizer nozzle. The surge line does not include any cast pipes or cast fittings. The welding processes used at the governing locations are Gas Tungsten Arc Weld (GTAW)/Shielded Metal Arc Weld (SMAW) combination. Figure 3-1 shows the schematic layout of the surge line and identifies the weld locations by node points.

In the following sections the tensile properties of the materials are presented for use in the Leak-Before-Break analyses.

3.2 MATERIAL PROPERTIES

R. E. Ginna Nuclear Power Plant specific data was used as a basis for determining tensile properties. The room temperature mechanical properties of the surge line material were obtained from the Certified Materials Test Reports (CMTRs) and are given in Table 3-1. The representative minimum and average tensile properties were established (see Table 3-2). The material properties at temperatures (255°F, 455°F, 617°F and 653°F) are required for the leak rate and stability analyses discussed later. The minimum and average tensile properties were calculated by using the ratio of the ASME Code Section II (Reference 3-1) properties at the temperatures of interest stated above. Table 3-2 shows the tensile properties at various temperatures. The moduli of elasticity values were established at various temperatures from the ASME Code Section II (see Table 3-3). In the Leak-Before-Break evaluation, the representative minimum yield strength and minimum ultimate strength at temperature were used for the flaw stability evaluations and the representative average yield strength was used for the leak rate predictions. These properties are summarized in Table 3-2.

3.3 REFERENCE

- 3-1 ASME Boiler and Pressure Vessel Code Section II, Part D – Material Properties, 2001 Edition, July 1, 2001, ASME Boiler and Pressure Vessel Committee, Subcommittee on Materials.

Table 3-1 Room Temperature Mechanical Properties of the Pressurizer Surge Line Materials

Heat #/Serial #	Material	Yield Strength (psi)	Ultimate Strength (psi)
D 8935/2165	SA376 TP316	36500	79000
D 8935/2165	SA376 TP316	38100	79000
D 8935/2167	SA376 TP316	36100	78000
D 8935/2167	SA376 TP316	37300	77200
D 8935/2168	SA376 TP316	34500	77800
D 8935/2168	SA376 TP316	38100	77400
D 6115/15	SA376 TP316	31000	75600
D 6115/15	SA376 TP316	34500	77300

Table 3-2 Representative Tensile Properties of the Pressurizer Surge Line Material

Material	Temperature (°F)	Minimum Yield (psi)	Average Yield (psi)	Minimum Ultimate (psi)
SA376 TP316	Room	31000	35763	75600
SA376 TP316	255	25296	29182	74436
SA376 TP316	455	21318	24593	72420
SA376 TP316	617	19389	22368	72374
SA376 TP316	653	19098	22032	72374

Table 3-3 Modulus of Elasticity (E) of the Pressurizer Surge Line Material

Temperature (°F)	E (ksi)
Room	28300
255	27270
455	26115
617	25215
653	25035

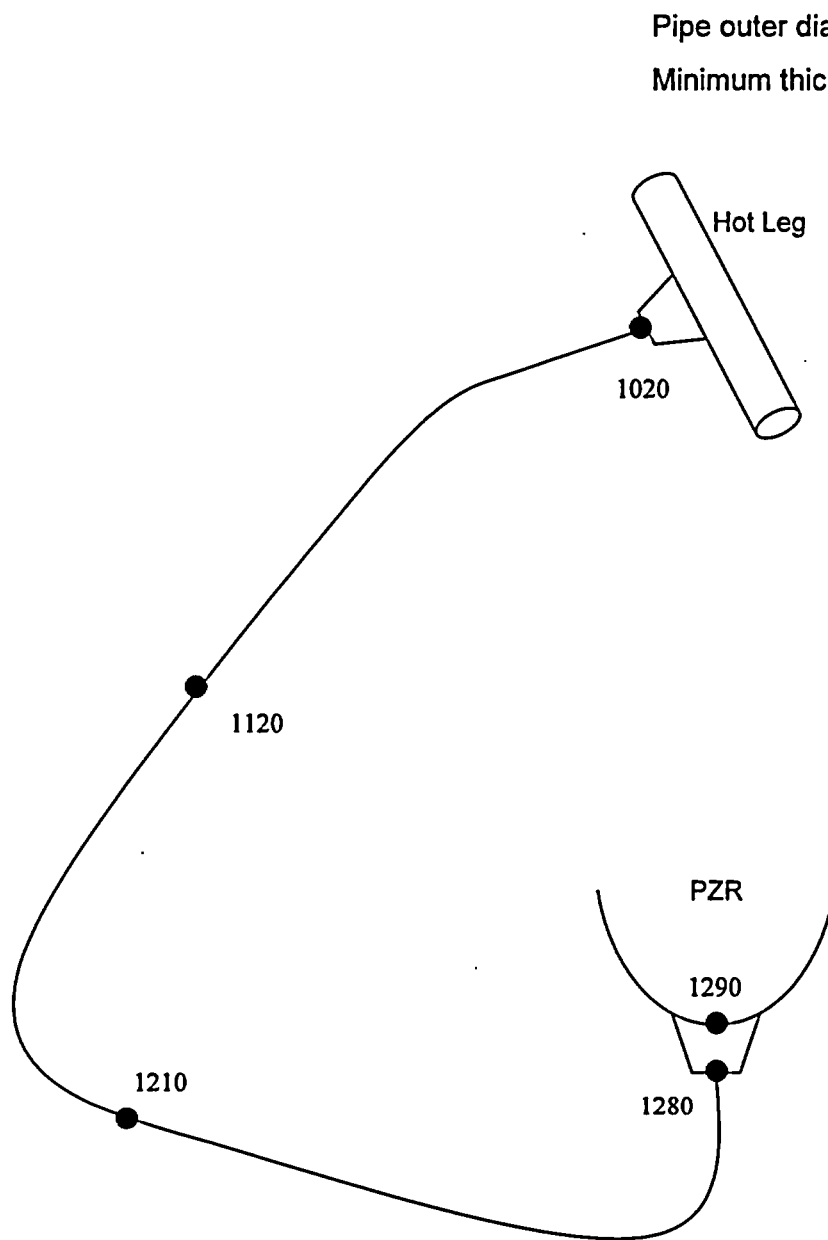


Figure 3-1 R. E. Ginna Nuclear Power Plant Surge Line Layout

4 LOADS FOR FRACTURE MECHANICS ANALYSIS

4.1 NATURE OF THE LOADS

Figure 3-1 shows a schematic layout of the surge line for the R. E. Ginna Nuclear Power Plant and identifies the weld locations.

The stresses due to axial loads and resultant moments were calculated by the following equation:

$$\sigma = \frac{F}{A} + \frac{M}{Z} \quad (4-1)$$

where,

σ	=	Stress
F	=	Axial Load
M	=	Resultant Moment
A	=	Metal Cross-Sectional Area
Z	=	Section Modulus

The moments for the desired loading combinations were calculated by the following equation:

$$M = (M_x^2 + M_y^2 + M_z^2)^{0.5} \quad (4-2)$$

where,

x axis is along the center line of the pipe.

M	=	Resultant Moment for Required Loading
M_x	=	Torsional Moment
M_y	=	Y Component of Bending Moment
M_z	=	Z Component of Bending Moment

The axial load and resultant moments for crack stability analysis and leak rate predictions are computed by the methods to be explained in Sections, 4.2 and 4.3 which follow.

4.2 LOADS FOR CRACK STABILITY ANALYSIS

In accordance with SRP 3.6.3 the absolute sum of loading components can be applied which results in higher magnitude of combined loads. If crack stability is demonstrated using these loads, the LBB margin can be reduced from $\sqrt{2}$ to 1.0. The faulted loads for the crack stability analysis were calculated by the absolute sum method as follows:

$$F = |F_{DW}| + |F_{TH}| + |F_P| + |F_{SSE}| \quad (4-3)$$

$$M_x = |M_{x,DW}| + |M_{x,TH}| + |M_{x,SSE}| \quad (4-4)$$

$$M_y = |M_{y,DW}| + |M_{y,TH}| + |M_{y,SSE}| \quad (4-5)$$

$$M_z = |M_{z,DW}| + |M_{z,TH}| + |M_{z,SSE}| \quad (4-6)$$

where

DW = Deadweight

TH = Applicable Thermal Expansion Load (Normal and applicable Stratified)

P = Load Due To Internal Pressure

SSE = Safe Shutdown Earthquake Loading (Note: there is no seismic anchor motion loads due to SSE in the surge line because the surge line was coupled with the loop in the piping stress analysis)

4.3 LOADS FOR LEAK RATE EVALUATION

The normal operating loads for leak rate predictions were calculated by the algebraic sum method as follows:

$$F = F_{DW} + F_{TH} + F_P \quad (4-7)$$

$$M_x = M_{x,DW} + M_{x,TH} \quad (4-8)$$

$$M_y = M_{y,DW} + M_{y,TH} \quad (4-9)$$

$$M_z = M_{z,DW} + M_{z,TH} \quad (4-10)$$

The parameters and subscripts are the same as those explained in Sections 4.1 and 4.2.

4.4 LOADING CONDITIONS

Because thermal stratification can cause large stresses during heatup and cooldown, a review of the stratification stresses was performed to identify the upper bound loadings. The loading states so identified are given in Table 4-1.

Seven loading cases were identified and are shown in Table 4-2. Cases A, B, C are the normal operating load cases and Cases D, E, F and G are the faulted load cases.

The cases postulated for Leak-Before-Break evaluation are summarized in Table 4-3. The cases of primary interest are the postulation of a detectable leak at normal 100% power [

] ^{a,c,e}

Case Combination [

] ^{a,c,e}

The case combination [

] ^{a,c,e}

The realistic cases [

] ^{a,c,e}

[

] ^{a,c,e}

4.5 SUMMARY OF LOADS

The combined loads were evaluated at the various weld locations. Normal loads were determined using the algebraic sum method whereas faulted loads were combined using the absolute sum method. Table 4-4 shows loads and stresses at the three highest stressed weld locations. For the entire surge line, the highest stress ratio between loading Case B and

Loading Case F also falls within these three weld locations. The minimum pipe wall thickness at the weld counter-bore was used in the analysis.

4.6 GOVERNING LOCATIONS

Node 1020 is the highest stress weld location in the R. E. Ginna Nuclear Power Plant surge line and this is the critical location. The second and third highest stress locations are at Nodes 1120 and Node 1280 respectively. LBB analyses were performed at these three locations. The weld processes used at these locations are GTAW/SMAW combinations.

Figure 4-1 shows the weld locations analyzed and identified by Node points. The loads and stresses at Nodes 1020, 1120 and 1280 are shown in Tables 4-4. Loads and stresses for Case C and Case G in Tables 4-4 are shown for information only and they are not used in the LBB analysis.

Table 4-1 Types of Loadings	
Pressure (P)	
Dead Weight (DW)	
Normal Operating Thermal Expansion (TH)	
Safe Shutdown Earthquake (SSE)	
[] a,c,e
[] a,c,e
[] a,c,e

A/D	This is the standard Leak-Before-Break evaluation.
A/F	This depicts a postulated forced cooldown event resulting from experiencing a detectable leak [] ^{a,c,e}
B/E	[] ^{a,c,e}
B/F	This depicts a postulated forced cooldown event resulting from experiencing a detectable leak [] ^{a,c,e}

Node	Case	F (kips)	Axial Stress (ksi)	M (in-kips)	Moment Stress (ksi)	Total stress (ksi)
1020	A	131.02	4.73	955.65	15.13	19.86
1020	B	131.18	4.73	985.93	15.61	20.34
1020	C	21.51	0.78	2351.62	37.23	38.01
1020	D	152.67	5.50	1183.75	18.75	24.25
1020	E	152.52	5.50	1231.07	19.49	24.99
1020	F	32.69	1.18	2351.62	37.23	38.41
1020	G	34.66	1.25	2595.73	41.10	42.35
1120	A	129.19	4.66	415.22	6.57	11.23
1120	B	129.37	4.66	546.14	8.65	13.31
1120	C	20.62	0.74	1538.46	24.36	25.10
1120	D	153.80	5.55	565.98	8.96	14.51
1120	E	153.62	5.54	700.69	11.09	16.63
1120	F	33.58	1.21	1540.12	24.39	25.60
1120	G	34.85	1.26	1650.33	26.13	27.39
1280	A	142.02	5.12	1108.85	17.56	22.68
1280	B	143.01	5.16	1031.95	16.34	21.50
1280	C	33.92	1.23	997.47	15.79	17.02
1280	D	146.59	5.29	1460.78	23.13	28.42
1280	E	145.65	5.25	1323.32	20.95	26.20
1280	F	33.92	1.22	997.47	15.80	17.02
1280	G	36.56	1.32	1350.56	21.38	22.70

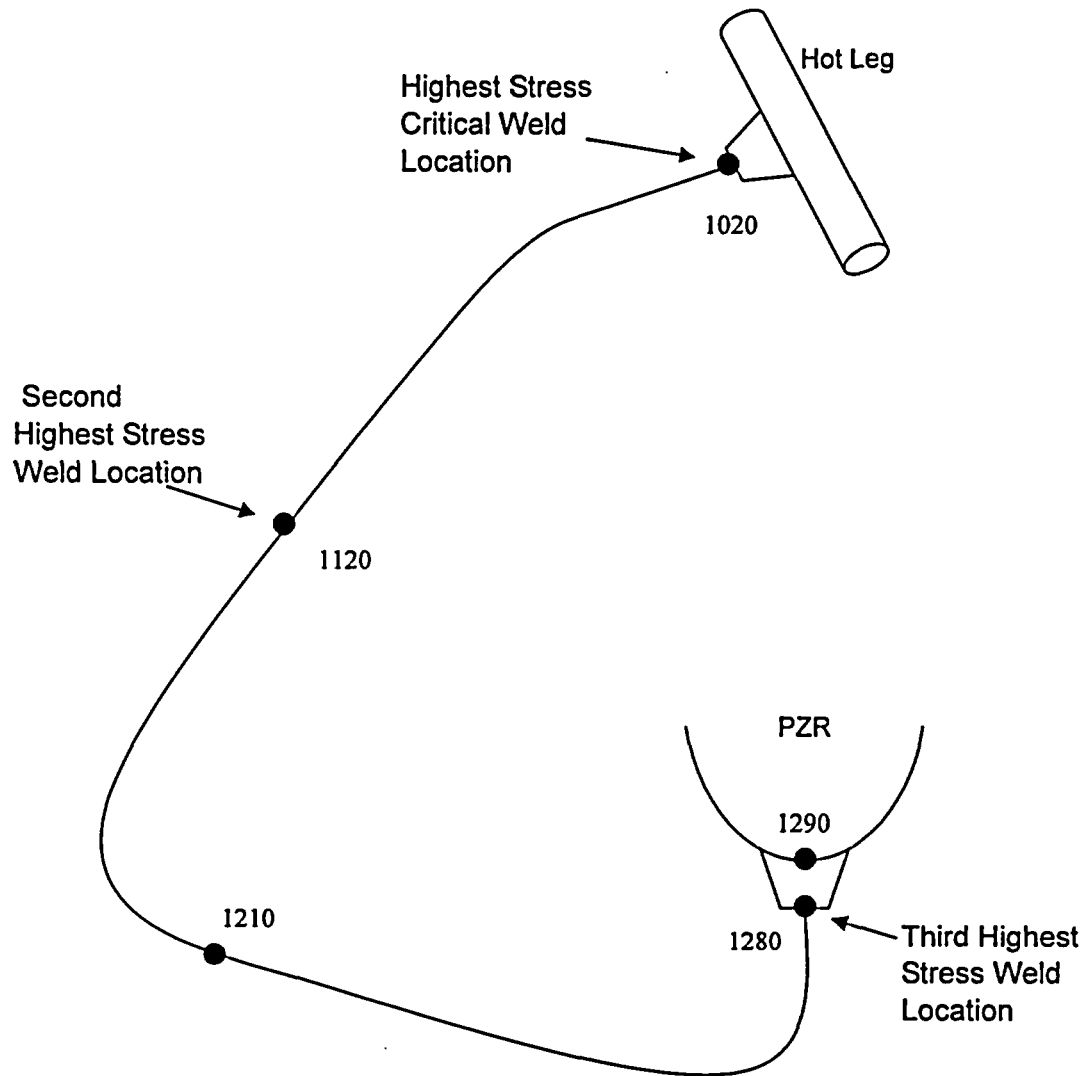


Figure 4-1 R. E. Ginna Nuclear Power Plant Surge Line Showing Analyzed Weld Locations by Node Point

5 FRACTURE MECHANICS EVALUATION

5.1 GLOBAL FAILURE MECHANISM

Determination of the conditions that lead to failure in stainless steel should be done with plastic fracture methodology because of the large amount of deformation accompanying fracture. One method for predicting the failure of ductile material is the []^{a,c,e} method based on traditional plastic limit load concepts, but accounting for []^{a,c,e} and taking into account the presence of a flaw. The flawed component is predicted to fail when the remaining net section reaches a stress level at which a plastic hinge is formed. The stress level at which this occurs is termed as the flow stress. []

[]^{a,c,e} This methodology has been shown to be applicable to ductile piping through a large number of experiments and is used here to predict the critical flaw size in the pressurizer surge line. The failure criterion has been obtained by requiring equilibrium of the section containing the flaw (Figure 5-1) when loads are applied. The detailed development is provided in Appendix A for a through-wall circumferential flaw in a pipe section with internal pressure, axial force, and imposed bending moments. The limit moment for such a pipe is given by:

$$[]^{\text{a,c,e}} \quad (5-1)$$

where:

[]

$$]^{\text{a,c,e}} \quad (5-2)$$

The analytical model described above accurately accounts for the internal pressure as well as an imposed axial force as they affect the limit moment. Good agreement was found between the analytical predictions and the experimental results (Reference 5-1). Flaw stability evaluations, using this analytical model, are presented in Section 5.3.

5.2 LEAK RATE PREDICTIONS

Fracture mechanics analysis shows that postulated through-wall cracks in the surge line would remain stable and would not cause a gross failure of this component. However, if such a through-wall crack did exist, it would be desirable to detect the leakage such that the plant could be brought to a safe shutdown condition. The purpose of this section is to discuss the method that will be used to predict the flow through such a postulated crack and present the leak rate calculation results for through-wall circumferential cracks.

5.2.1 General Considerations

The flow of hot pressurized water through an opening to a lower backpressure (causing choking) is taken into account. For long channels where the ratio of the channel length, L , to hydraulic diameter, D_H , (L/D_H) is greater than []^{a,c,e}, both []^{a,c,e} must be considered. In this situation, the flow can be described as being single-phase through the channel until the local pressure equals the saturation pressure of the fluid. At this point, the flow begins to flash and choking occurs. Pressure losses due to momentum changes will dominate for []^{a,c,e}. However, for large L/D_H values, the friction pressure drop will become important and must be considered along with the momentum losses due to flashing.

5.2.2 Calculation Method

In using the []

]a,c,e.

The flow rate through a crack was calculated in the following manner. Figure 5-2 from Reference 5-3 was used to estimate the critical pressure, P_c , for the primary loop enthalpy condition and an assumed flow. Once P_c was found for a given mass flow, the []

]a,c,e was found from Figure 5-3 taken from Reference 5-3. For all cases considered, since []

]a,c,e Therefore, this method will yield the two-phase pressure drop due to momentum effects as illustrated in Figure 5-4. Now using the assumed flow rate, G , the frictional pressure drop can be calculated using

$$\Delta P_f = []^{a,c,e} \quad (5-3)$$

where the friction factor f was determined using the []^{a,c,e} The crack relative roughness, ϵ , was obtained from fatigue crack data on stainless steel samples. The relative roughness value used in these calculations was []^{a,c,e} RMS.

The frictional pressure drop using Equation 5-3 was then calculated for the assumed flow and added to the []^{a,c,e} to obtain the total pressure drop from the system under consideration to the atmosphere. Thus,

$$\text{Absolute Pressure} - 14.7 = []^{\text{a,c,e}} \quad (5-4)$$

for a given assumed flow G. If the right-hand side of Equation 5-4 does not agree with the pressure difference between the piping under consideration and the atmosphere, then the procedure is repeated until Equation 5-4 is satisfied to within an acceptable tolerance and these results in the flow value through the crack.

5.2.3 Leak Rate Calculations

Leak rate calculations were performed as a function of postulated through-wall crack length for the three locations previously identified. The crack opening area was estimated using the method of Reference 5-4 and the leak rates were calculated using the calculation methods described above. The leak rates were calculated using the normal operating loads at the governing locations identified in Section 4.0. Average yield strength properties shown in Table 3-2 were used for the leak rate calculation. The crack lengths yielding a leak rate of 2.5 gpm (10 times the leak detection capability of 0.25 gpm) for the three locations in the R. E. Ginna Nuclear Power Plant pressurizer surge line are shown in Table 5-1.

The R. E. Ginna Nuclear Power Plant has a RCS pressure boundary leak detection system capable of detecting a leakage of 0.25 gpm in one hour (Reference 5-5).

5.3 STABILITY EVALUATION

A typical segment of the pipe under maximum loads of axial force F and bending moment M is schematically illustrated in Figure 5-5. In order to calculate the critical flaw size, plots of the limit moment versus crack length are generated as shown in Figures 5-6 to 5-14. The critical flaw size corresponds to the intersection of this curve and the maximum load line. The critical flaw sizes are calculated using the lower bound base metal tensile properties shown in Table 3-2.

The welds at the governing locations are GTAW/SMAW combination. The "Z" factor for GTAW is 1.0 and therefore, the "Z" factor correction for the SMAW was applied (Reference 5-6) as follows:

$$Z = 1.15 [1 + 0.013 (OD - 4)] \quad (\text{for SMAW}) \quad (5-5)$$

where OD is the outer diameter in inches. Substituting OD = 10.75 inches, the Z factor was calculated to be 1.251 for SMAW. The applied loads were increased by the applicable Z factor and the plots of limit load versus crack length were generated as shown in Figures 5-6 to 5-14. Table 5-2 shows the summary of critical flaw sizes.

5.4 REFERENCES

- 5-1 Kanninen, M. F. et al., "Mechanical Fracture Predictions for Sensitized Stainless Steel Piping with Circumferential Cracks" EPRI NP-192, September 1976.
- 5-2 []
]a,c,e
- 5-3 M. M. El-Wakil, "Nuclear Heat Transport "International Textbook Company, New York, N.Y, 1971.
- 5-4 Tada, H., "The Effects of Shell Corrections on Stress Intensity Factors and the Crack Opening Area of Circumferential and a Longitudinal Through-Crack in a Pipe," Section II-1, NUREG/CR-3464, September 1983.
- 5-5 Table 5.2-5 (Reactor Coolant Pressure Boundary to Containment Leakage Detection Systems) of Ginna UFSAR Revision 18.
- 5-6 Standard Review Plan; Public Comment Solicited; 3.6.3 Leak-Before-Break Evaluation Procedures; Federal Register/Vol. 52, No. 167/Friday, August 28, 1987/Notices, pp. 32626-32633.

Table 5-1 Summary of Leakage Flow Sizes			
Node Point	Load Case	Temperature (°F)	Leakage Flow Size (in.) (for 2.5 gpm leakage)
1020	A	653	1.61
1020	B	[] ^{a,c,e}	1.53
1120	A	653	2.68
1120	B	[] ^{a,c,e}	2.30
1280	A	653	1.38
1280	B	[] ^{a,c,e}	1.47

Table 5-2 Summary of Critical Flaw Sizes			
Node Point	Load Case	Temperature (°F)	Critical Flaw Size (in)
1020	D	653	9.02
1020	E	[] ^{a,c,e}	8.82
1020	F	[] ^{a,c,e}	5.58
1120	D	653	12.28
1120	E	[] ^{a,c,e}	11.54
1120	F	[] ^{a,c,e}	9.65
1280	D	653	7.76
1280	E	[] ^{a,c,e}	8.44
1280	F	[] ^{a,c,e}	12.31

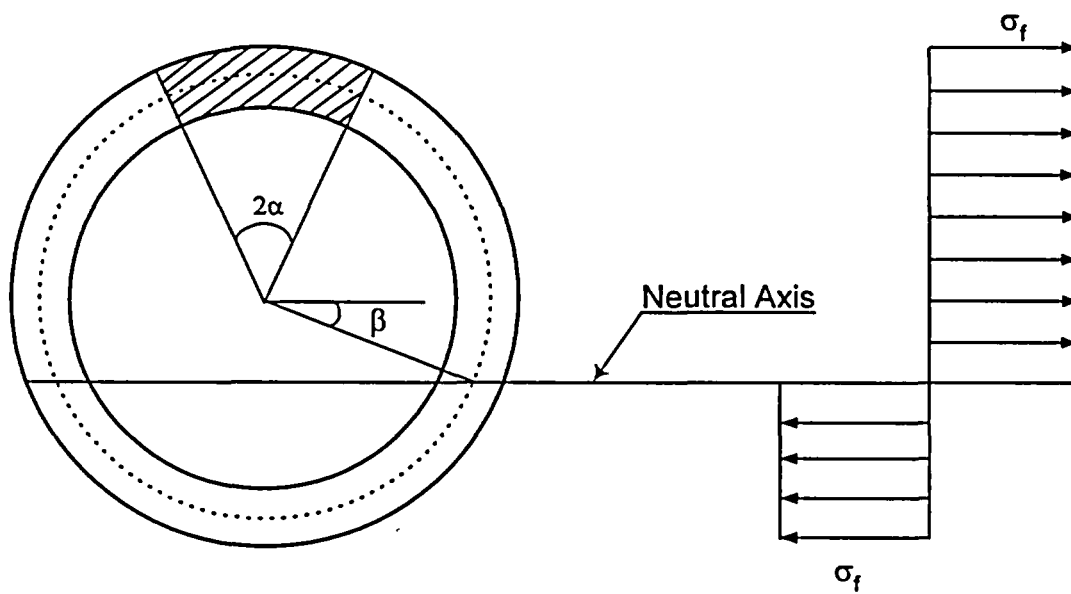


Figure 5-1 Fully Plastic Stress Distribution

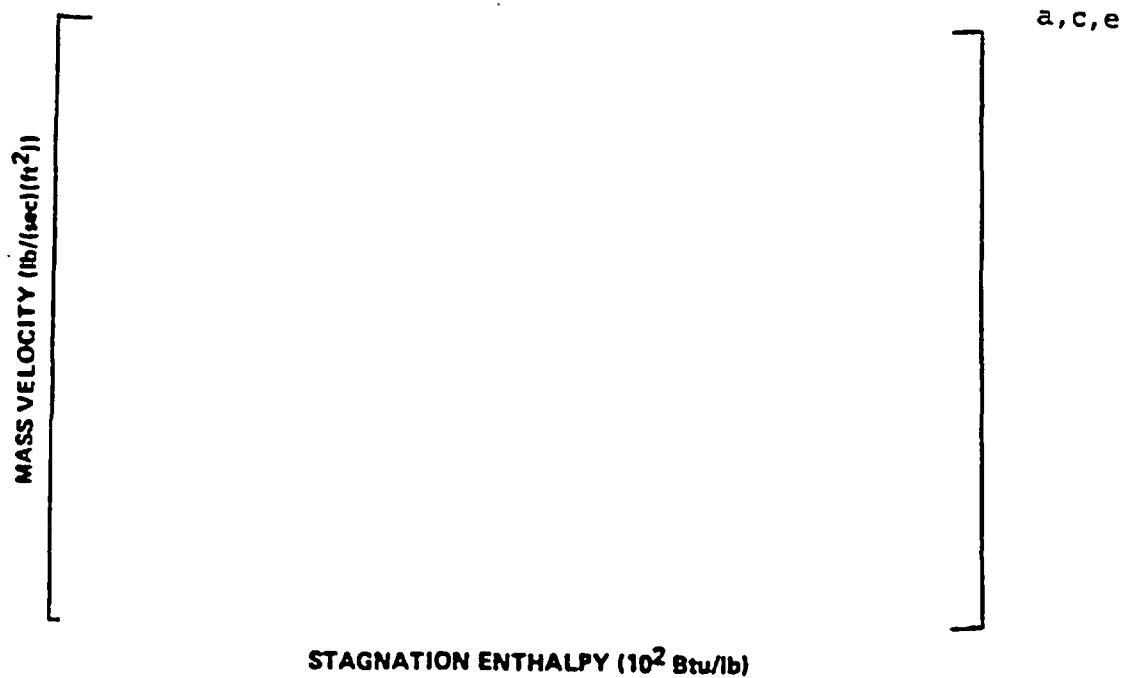


Figure 5-2 Analytical Predications of Critical Flow Rates of Steam-Water Mixtures

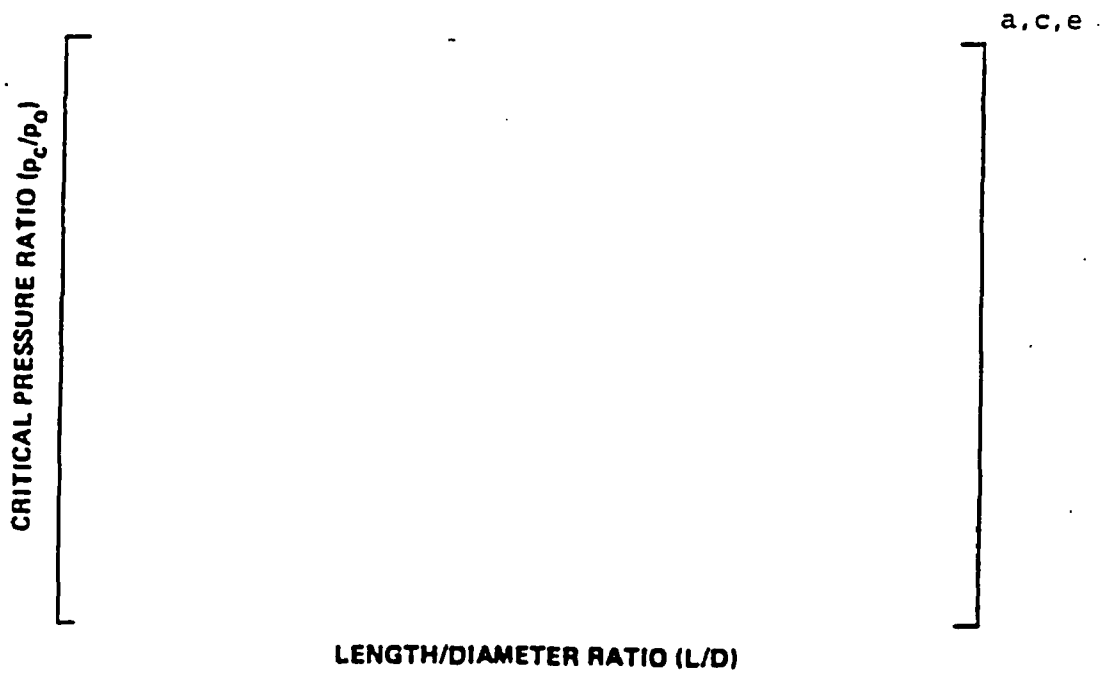


Figure 5-3 [

]a,c,e Pressure Ratio as a Function of L/D

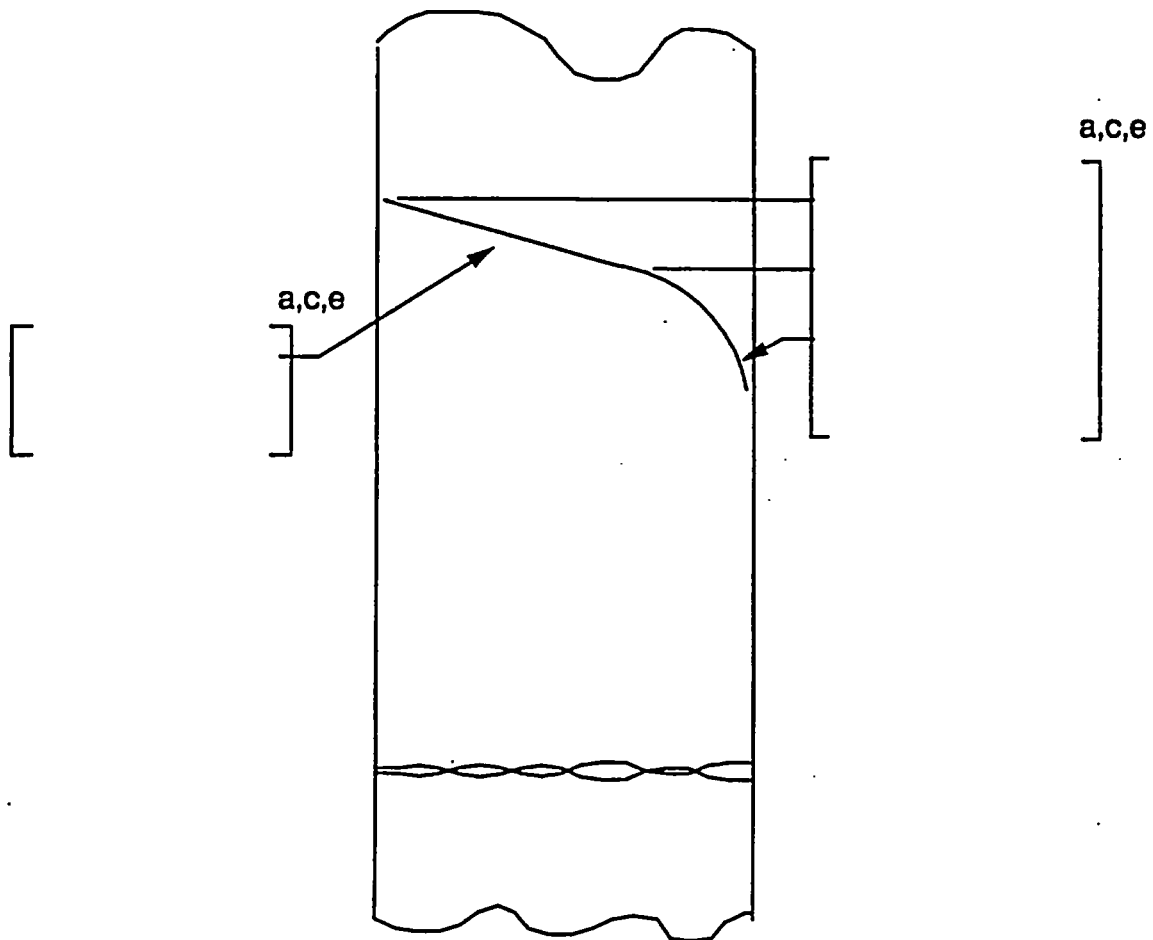


Figure 5-4 Idealized Pressure Drop Profile through a Postulated Crack

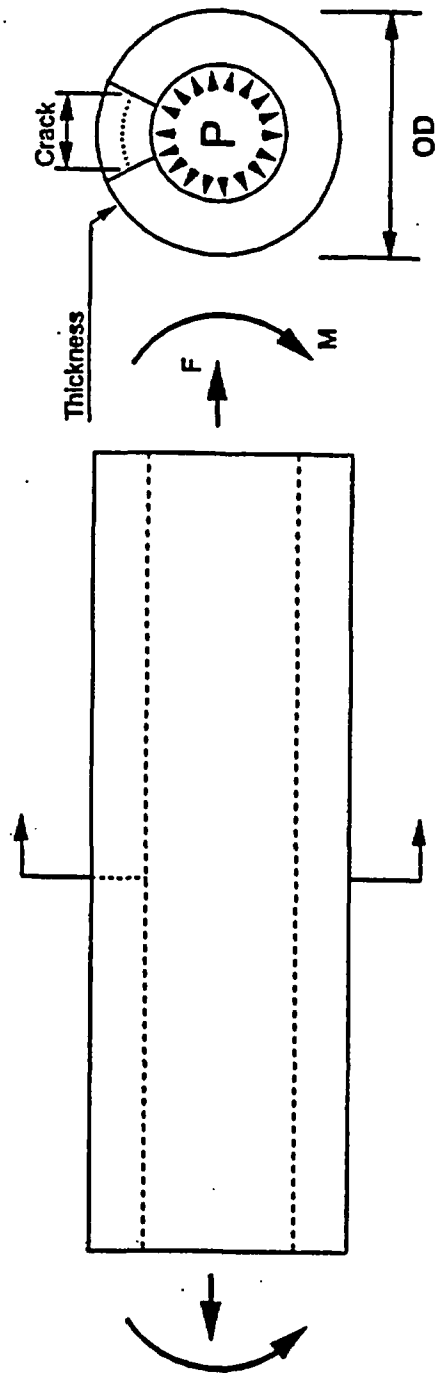


Figure 5-5 Loads acting on the Model at the Governing Locations

a,c,e

OD = 10.75 in $\sigma_y = 19.098$ ksi F = 152.67 kips
t = 0.896 in $\sigma_u = 72.374$ ksi M = 1183.75 in-kips
SA376 TP316 with SMAW weld

Figure 5-6 Critical Flaw Size Prediction for Node 1020 Case D

a,c,e

OD = 10.75 in $\sigma_y = 19.389$ ksi F = 152.52 kips
t = 0.896 in $\sigma_u = 72.374$ ksi M = 1231.07 in-kips
SA376 TP316 with SMAW weld

Figure 5-7 Critical Flaw Size Prediction for Node 1020 Case E

a,c,e

OD = 10.75 in $\sigma_y = 25.296$ ksi F = 32.69 kips
t = 0.896 in $\sigma_u = 74.436$ ksi M = 2351.62 in-kips
SA376 TP316 with SMAW weld

Figure 5-8 Critical Flaw Size Prediction for Node 1020 Case F

a,c,e

OD = 10.75 in $\sigma_y = 19.098$ ksi F = 153.80 kips
t = 0.896 in $\sigma_u = 72.374$ ksi M = 565.98 in-kips
SA 376 TP316 with SMAW weld

Figure 5-9 Critical Flaw Size Prediction for Node 1120 Case D

a,c,e

OD = 10.75 in $\sigma_y = 19.389$ ksi F = 153.62 kips
t = 0.896 in $\sigma_u = 72.374$ ksi M = 700.69 in-kips
SA 376 TP316 with SMAW weld

Figure 5-10 Critical Flaw Size Prediction for Node 1120 Case E

a,c,e

OD = 10.75 in $\sigma_y = 25.296$ ksi F = 33.58 kips
t = 0.896 in $\sigma_u = 74.436$ ksi M = 1540.12 in-kips
SA 376 TP316 with SMAW weld

Figure 5-11 Critical Flaw Size Prediction for Node 1120 Case F

a,c,e

OD = 10.75 in $\sigma_y = 19.098$ ksi F = 146.59 kips
t = 0.896 in $\sigma_u = 72.374$ ksi M = 1460.78 in-kips
SA376 TP316 with SMAW weld

Figure 5-12 Critical Flaw Size Prediction for Node 1280 Case D



OD = 10.75 in $\sigma_y = 19.098$ ksi F = 145.65 kips
t = 0.896 in $\sigma_u = 72.374$ ksi M = 1323.32 in-kips
SA376 TP316 with SMAW weld

Figure 5-13 Critical Flaw Size Prediction for Node 1280 Case E



OD = 10.75 in

$\sigma_y = 21.318$ ksi

F = 33.92 kips

t = 0.896 in

$\sigma_u = 72.420$ ksi

M = 997.47 in-kips

SA376 TP316 with SMAW weld

Figure 5-14 Critical Flaw Size Prediction for Node 1280 Case F

6 ASSESSMENT OF FATIGUE CRACK GROWTH

6.1 METHODOLOGY

To determine the sensitivity of the pressurizer surge line to the presence of postulated small cracks when subjected to the various transients, a Fatigue Crack Growth (FCG) analysis was performed.

The methodologies consists of first obtaining the local and structural transient stress analyses results and then superimpose them to obtain the total stresses. The design cycles used in the FCG analyses were the same ones (including OBE) that were used in Reference 6-1 for the cumulative usage factor calculations. An initial flaw size was postulated and the calculation of crack growth for the design plant life (60 years) using the austenitic stainless steel crack growth law was performed. The fatigue crack growth analysis was performed in the surge line pipe close to the reducer (where a maximum cumulative usage factor occurred as shown in Reference 6-1). Five through wall angular locations on the cross-section of the pipe were analyzed and their orientations are shown in Figure 6-1.

There is presently no fatigue crack growth curve in the ASME Code for austenitic stainless steels in a water environment. However, a great deal of work has been done that supports the development of such a curve. An extensive study was performed by the Materials Property Council Working Group on Reference Fatigue Crack Growth concerning the crack growth behavior of Austenitic stainless steel in an air environment, published in Reference 6-2. A reference fatigue crack growth curve for stainless steel in an air environment, based on this work, appears in Appendix C of the ASME Section XI Code, 2001 Edition (Reference 6-3). This curve is shown in Figure 6-2.

A compilation of data for austenitic stainless steel in a PWR water environment was made by Bamford (Reference 6-4), and it was found that the effect of the environment on the crack growth rate was small. For this reason it was conservatively estimated that the environmental factor should be set at []^{a,c,e} in the crack growth rate equation from Reference 6-2. Based on these works (References 6-2 and 6-4) the stainless steel fatigue crack growth law used in the analyses is:

[

J^{a,c,e}

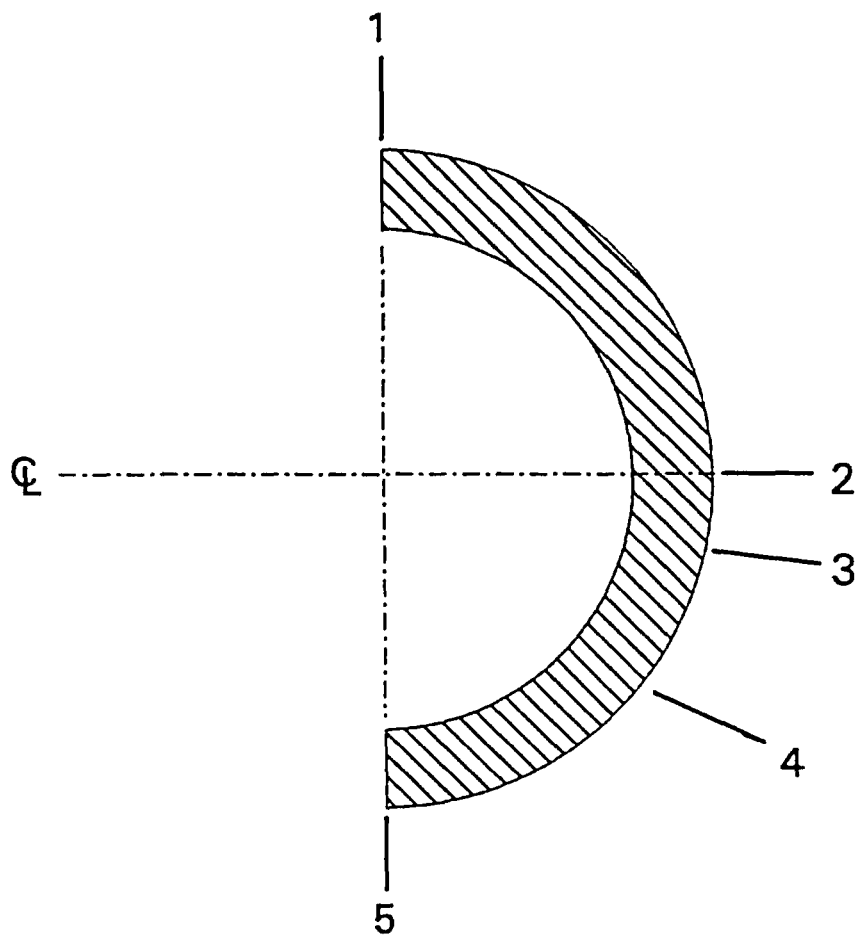
6.2 RESULTS

Fatigue crack growth analyses were carried out along five angular locations (Figure 6-1) on the cross-section of the pipe. At each angular location stresses for each transient were obtained along with the number of cycles for input into fatigue crack growth analysis. The analyses were completed for postulated initial flaws oriented circumferentially. The flaws were assumed to be semi-elliptical with an aspect ratio of six to one. The initial flaw sizes were assumed to be 10% of the wall thickness. The results of the fatigue crack growth analyses are presented in Table 6-1. For an initial flaw size of 0.0896 inch, which is 10 percent of the minimum wall thickness, the result shows that the maximum final flaw size after 60 years is about 13.9% of the minimum wall thickness. Therefore flaw growth through the wall is not expected to occur during the 60 year design life of the plant and it is concluded that fatigue crack growth is not be a concern for the R.E. Ginna pressurizer surge line.

Note: R.E. Ginna pressurizer surge line 60 years design transients and cycles are the same as those of 40 years and therefore, FCG results for 40 years and 60 years are the same.

6.3 REFERENCES

- 6-1 "Structural Evaluation of Robert E. Ginna Pressurizer Surge Line, Considering the Effects of Thermal Stratification," WCAP-12928, May 1991 (Westinghouse Proprietary).
- 6-2 James, L. A. and Jones, D. P., "Fatigue Crack Growth Correlations for Austenitic Stainless Steel in Air," in Predictive Capabilities in Environmentally Assisted Cracking, ASME publication PVP-99, December 1985.
- 6-3 ASME Boiler and Pressure Vessel Code Section XI, 2001 Edition, "Rules for Inservice Inspection of Nuclear Power Plant Components"
- 6-4 Bamford, W. H., "Fatigue Crack Growth of Stainless Steel Reactor Coolant Piping in a Pressurized Water Reactor Environment," ASME Trans. Journal of Pressure Vessel Technology, February 1979.



Half Cross-section of the Pipe

Figure 6-1 **Orientation of Angular Locations for the Fatigue Crack Growth Analysis**

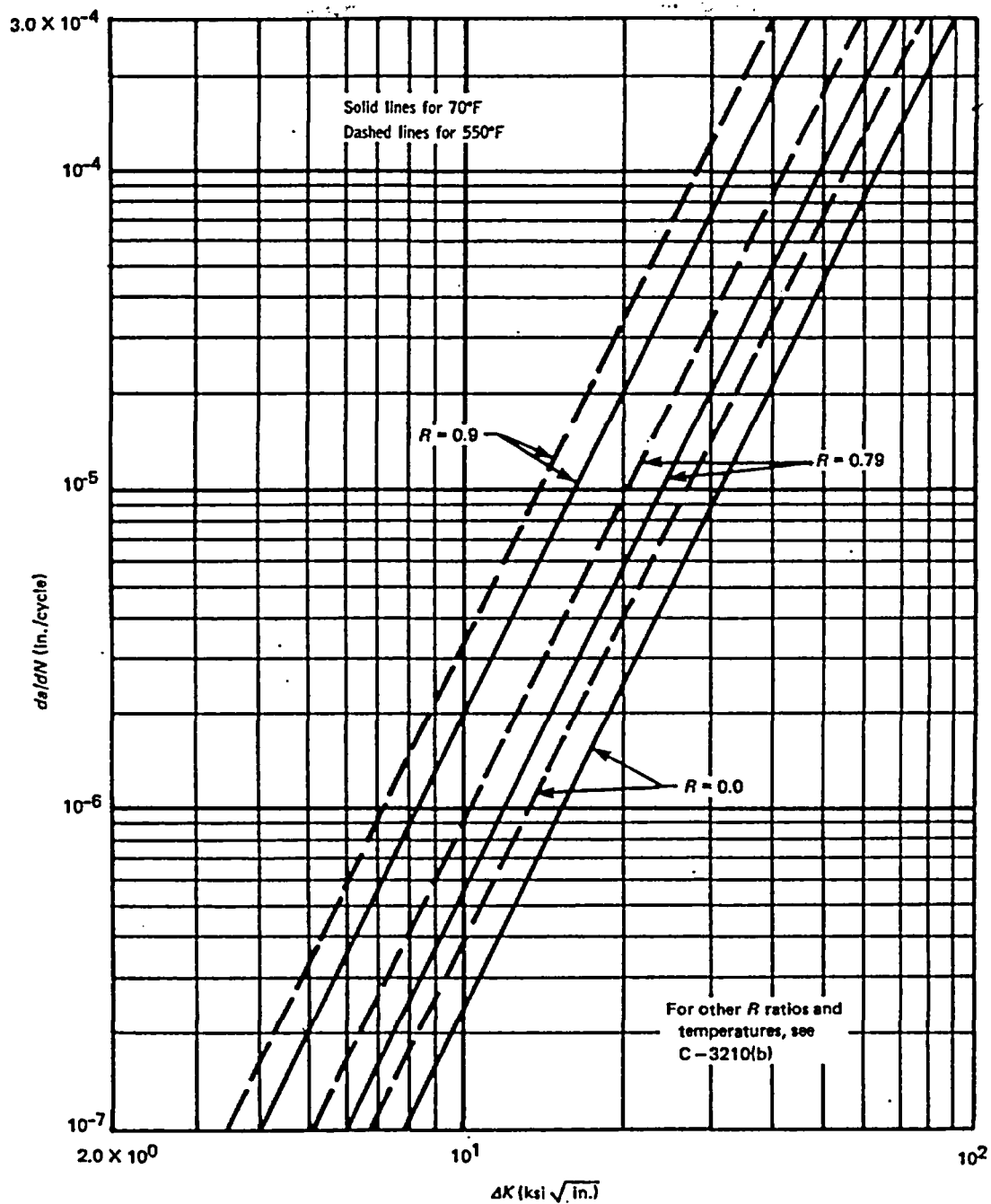


Figure 6-2 Reference Fatigue Crack Growth Curves for Austenitic Stainless Steel in Air Environments

7 ASSESSMENT OF MARGINS

In the preceding sections, the leak rate calculations, fracture mechanics analysis and fatigue crack growth assessment were performed. In Section 5.3 using the SRP 3.6.3 approach (i.e., "Z" factor approach), the "critical" flaw sizes at the governing locations are calculated. In Section 5.2 the crack lengths yielding a leak rate of 2.5 gpm (10 times the leak detection capability of 0.25 gpm) for the governing locations are calculated. Margins at these locations are summarized below:

- **Margin on Leak Rate:**

A margin of 10 exists between the calculated leak rate from the leakage flaw and the leak detection capability of 0.25 gpm.

- **Margin on Flaw Size:**

Using faulted loads obtained by the absolute sum method, a margin of 2 or more exists between the critical flaw and the flaw having a leak rate of 2.5 gpm (the leakage flaw). The margins for analysis combination cases A/D, A/F, B/E, B/F well exceed the factor of 2.

- **Margin On loads:**

The faulted loads are combined by absolute summation method and therefore the recommended margin on loads of 1.0 is satisfied as per SRP 3.6.3.

The leakage flaw sizes, the critical flaw sizes, and the margins are given in Table 7-1. The margins are the ratio of critical flaw size to leakage flaw size. All the LBB recommended margins are satisfied.

In this evaluation, the Leak-Before-Break methodology is applied conservatively. The conservatisms used in the evaluation are summarized in Table 7-2.

Table 7-1 Leakage Flaw Sizes, Critical Flaw Sizes and Margins				
Node	Load Case	Critical Flaw Size (in)	Leakage Flaw Size (in)	Margin
1020	A/D	9.02	1.61	5.60
1020	A/F	5.58	1.61	3.47
1020	B/E	8.82	1.53	5.76
1020	B/F	5.58	1.53	3.65
1120	A/D	12.28	2.68	4.58
1120	A/F	9.65	2.68	3.60
1120	B/E	11.54	2.30	5.02
1120	B/F	9.65	2.30	4.20
1280	A/D	7.76	1.38	5.62
1280	A/F	12.31	1.38	8.92
1280	B/E	8.44	1.47	5.74
1280	B/F	12.31	1.47	8.37

Table 7-2 Leak-Before-Break Conservatisms
Factor of 10 on Leak Rate
Factor of 2 on Leakage Flaw
Algebraic Sum of Loads for Leakage
Absolute Sum of Loads for Stability
Average Material Properties for Leakage
Minimum Material Properties for Stability

8 CONCLUSIONS

This report justifies the elimination of pressurizer surge line pipe breaks as the structural design basis for the R. E. Ginna Nuclear Power Plant as follows:

- a. Stress corrosion cracking is precluded by use of fracture resistant materials in the piping system and controls on reactor coolant chemistry, temperature, pressure, and flow during normal operation.

Note: As a result of the recent issue of Primary Water Stress Corrosion Cracking (PWSCC) occurring in V. C. Summer reactor vessel hot leg nozzle, Alloy 82/182 weld is being currently investigated under the EPRI Materials Reliability Project (MRP) Program. It should be noted that the susceptible material under investigation is not found in the pressurizer surge line piping at the R. E. Ginna Nuclear Power Plant.

- b. Water hammer should not occur in the RCS piping (primary loop and the attached class 1 auxiliary line) because of system design, testing, and operational considerations.
- c. The effects of low and high cycle fatigue on the integrity of the surge line were evaluated and shown acceptable. The effects of thermal stratification were evaluated and shown acceptable.
- d. Ample margin exists between the leak rate of small stable flaws and the capability of the R. E. Ginna Nuclear Power Plant reactor coolant system pressure boundary leakage detection system(margin on leak rate of 10 was satisfied, see Table 5-1).
- e. Ample margin exists between the small stable leakage flow sizes of item (d) and the critical flow sizes (see Table 7-1 for a summary of margin).

The postulated reference flaw will be stable because of the ample margins in items (d) and (e), and will leak at a detectable rate which will assure a safe plant shutdown.

Based on the above, it is concluded that pressurizer surge line breaks should not be considered in the structural design basis of the R. E. Ginna Nuclear Power Plant.

APPENDIX A - LIMIT MOMENT

[

] a,c,e



Figure A-1 Pipe With A Through-Wall Crack In Bending